Late Pleistocene charcoal-rich sediments in the Puerto Rico Trench, possible remnants of gigantic wildfires in North-Eastern South America

Chloé Seibert, Christian Beck, Nathalie Feuillet, Eva Moreno, Denise Pons, Chris Goldfinger, Gueorgui Ratzov, Guillaume St-Onge, Arthur Bieber, Pierre Morena, et al.

Palaeogeography, Palaeoclimatology, Palaeoecology 655 (2024) 112497

Contents lists available at ScienceDirect

Palaeogeography, Palaeoclimatology, Palaeoecology

journal homepage: www.elsevier.com/locate/palaeo

Late Pleistocene charcoal-rich sediments in the Puerto Rico Trench, possible remnants of gigantic wildfires in North-Eastern South America

Chloé Seibert [a,b,*], Christian Beck [c], Nathalie Feuillet [a], Eva Moreno [d], Denise Pons [e], Chris Goldfinger [f], Gueorgui Ratzov [g], Guillaume St-Onge [h], Arthur Bieber [h], Pierre Morena [g], Jason Patton [i], Valentina Batanova [c], René Maury [j]

[a] Université de Paris Cité, Institut de Physique du Globe de Paris, CNRS, Paris, France
[b] Lamont-Doherty Earth Observatory, Columbia University, Palisades, NY, United States of America
[c] Univ. Grenoble Alpes, Univ. Savoie-Mont-Blanc, CNRS, IRD, Univ. Gustave Eiffel ISTerre, 38000 Grenoble, France
[d] Laboratoire d'Océanographie et du Climat (LOCEAN), CNRS, IRD, MNHN, Sorbonne Université, Paris, France
[e] Sorbonne Université, UPMC Univ. Paris 06, CNRS, MNHN, UMR 7207 (CR2P), 75231 Paris, France
[f] College of Earth, Ocean, and Atmospheric Sciences, Oregon State University, Corvallis, OR, USA
[g] Université Côte d'Azur, CNRS, IRD, Observatoire de la Côte d'Azur, Géoazur, Nice, France
[h] Institut des Sciences de la mer (ISMER), Chaire de Recherche du Canada en Géologie Marine, Université du Québec à Rimouski et GEOTOP, Canada
[i] Humbolt State University, USA
[j] Géo-Océan, Université de Bretagne Occidentale, Brest, France

ARTICLE INFO

Editor: Howard Falcon-Lang

Keywords:
Guyana shield
Wood-fire
Barbados prism
Puerto Rico Trench
Sediment transfer

ABSTRACT

An 18,000 km^2 area of the Guyana Shield of South America, known as the Gran Sabana, is characterized by savannah vegetation that contrasts strongly with surrounding rain forests. Its origin has been linked to multiple episodes of forest fires. In this paper, we report a deposit encountered in two piston cores sampled during the CASEIS marine cruise, at 6000 m-depth at the southern entrance of the Puerto Rico Trench. The existence of this deposit call into question our understanding of the evolution of the Gran Sabana. We sampled its upper ~60 cm, which comprises leaves and wood fragments, seeds, and charcoal, intermixed with siliciclastic sediment of igneous-metamorphic continental provenance. Radiocarbon dates of the vegetal fragments and charcoal range between 30 and 23 kyr BP. We propose that these deep ocean charcoal-rich sediments, located 2500 km offshore from the Orinoco Delta, may be remnants of gigantic forest fires of the Guyana Shield. We infer that this material was eroded during an extreme regional rainfall event, transported down rivers during one or more episodes to the Orinoco delta, and then travelled offshore via a deep turbiditic submarine system flowing on the Atlantic seafloor. It finally reached the Puerto Rico Trench, forming what we term, the Baracuda Trench Debrite. While published paleoclimatic analyses of lacustrine sediments have suggested that the Gran Sabana originated during episodes of wildfire ~12.5 kyr BP ago, radiocarbon dating of Baracuda Trench Debrite suggests the occurrence of earlier fires in this region, leading us to re-evaluate the age of the Gran Sabana. These fires occurred during the low glacial maximum (LGM) and were likely promoted by climate change.

1. Introduction

Late Quaternary paleoclimatic evolution of northern South-America is driven by the changing position of the Intertropical Convergence Zone (ITCZ) (e.g. Haug et al., 2001; Peterson and Haug, 2004). This basically involves hydrological changes. From a recent global synthesis, Bradley and Diaz (2021a and 2021b) defined Tropical Hydrologic Events (THE) as abrupt and strong changes from sun overhead to rainfall periods, resulting from the southward displacement of the ITCZ related to northern climate changes. Alternate situations are severe drought inferred to favour large wood-fires (Salgado-Labouriau, 1997; Siffedine et al., 2001, 2003; Montoya et al., 2011a; Ballesteros et al., 2014; Hoffmann et al., 2014; Rull et al., 2015), sometimes leading to near-surface vitrifications (Roperch et al., 2017). The Guyana Shield, which corresponds to a high part (~1000 m mean altitude) of the South American craton, lies between the Orinoco and Amazon rivers. It is

* Corresponding author at: Université de Paris Cité, Institut de Physique du Globe de Paris, CNRS, Paris, France.
E-mail address: cseibert@ldeo.columbia.edu (C. Seibert).

https://doi.org/10.1016/j.palaeo.2024.112497
Received 11 June 2024; Received in revised form 6 September 2024; Accepted 6 September 2024
Available online 8 September 2024

presently undergoing tropical climatic conditions, and covered by a rainforest, except a large area called the "Gran Sabana". This juxtaposition of two different vegetal covers has been previously investigated, focusing on a possible replacement of rainforest by savannah due to climate changes (Montoya et al., 2011a; Montoya et al., 2011b; Ballesteros et al., 2014; Rull et al., 2015). Based on pollen records and charcoal occurrences in small lakes fills, Rull et al. (2015) conclude that a "savannisation" developed between 12.5 and 13.0 kyr BP (Younger Dryas). They detected, at one site, several charcoal abundance peaks during this period, and, on another site, a unique major occurrence between 12.0 and 12.5 kyr. Parts of these different works attribute a natural origin (severe drought) to the 13.0-to-12.0 kyr BP charcoal occurrence, and to a rapid rainforest disappearance, and consider later minor occurrences of charcoal as consequences of traditional anthropogenic practices. Rull et al. (2015) envisaged an earlier (Younger Dryas-Holocene limit) anthropic triggering.

During the CASEIS oceanographic cruise (Feuillet, 2016; Seibert et al., 2020; Morena et al., 2022), we sampled a layer reworking abundant charcoal and vegetal fragments at 6000 m water depth at the entrance of the Puerto Rico trench off the islands of the Lesser Antilles arc. From the analysis of this layer content, we suspected that this material might originate from the Guyana shield and could be a remnant of forest fires following a major drought episode. We investigate this hypothesis, the age of the deposit and its possible relationships with a Late Pleistocene climatic episode which affected the northern South-America continent.

2. Geological setting

2.1. Lesser Antilles subduction zone

The Puerto-Rico and Lesser Antilles trench results from the subduction of the North and South American lithospheric plates beneath the Caribbean at a rate of 2 cm/yr (Symithe et al., 2015) and lies against the one of the largest known accretionary wedges worldwide: the Barbados Prism (Fig. 1) (Speed, 1981; Biju-Duval et al., 1982; Mascle and Moore, 1990). This wedge is up to 240 km wide and 15 km thick and has been built since the Late Paleocene by accretion of a thick sedimentary cover. It is mainly composed of a large amount of terrigenous material originating from the South-American continent since the Late Paleocene (Larue and Speed, 1983; Dolan et al., 1989; Stéphan et al., 1990; Beck et al., 1990; Capet et al., 1990). The morphology of the accretionary wedge is controlled by the subduction of two main oceanic ridges (Barracuda and Tiburon, Dolan et al., 1989, Patriat et al., 2011; Pichot et al., 2012). The ridges deformed both the wedge and the frontal margin (Bénâtre et al., 2022) and acted as dam retaining the sediments from south-America. As a result, the accretionary wedge is very thick south of the ridges and narrows northwards, at the eastern entrance of the Puerto Rico Trench. The way in which sediments are transferred from South America to feed the Barbados wedge has been studied by several authors (e.g. Deville et al., 2006, 2015; Padrón de Carrillo, 2007; Callec et al., 2010). Presently, the sediments are originating from the Orinoco Delta and travel over long distance via oceanic bottom currents following a complex system of canyons and channels (Yellow lines on Fig. 1). The

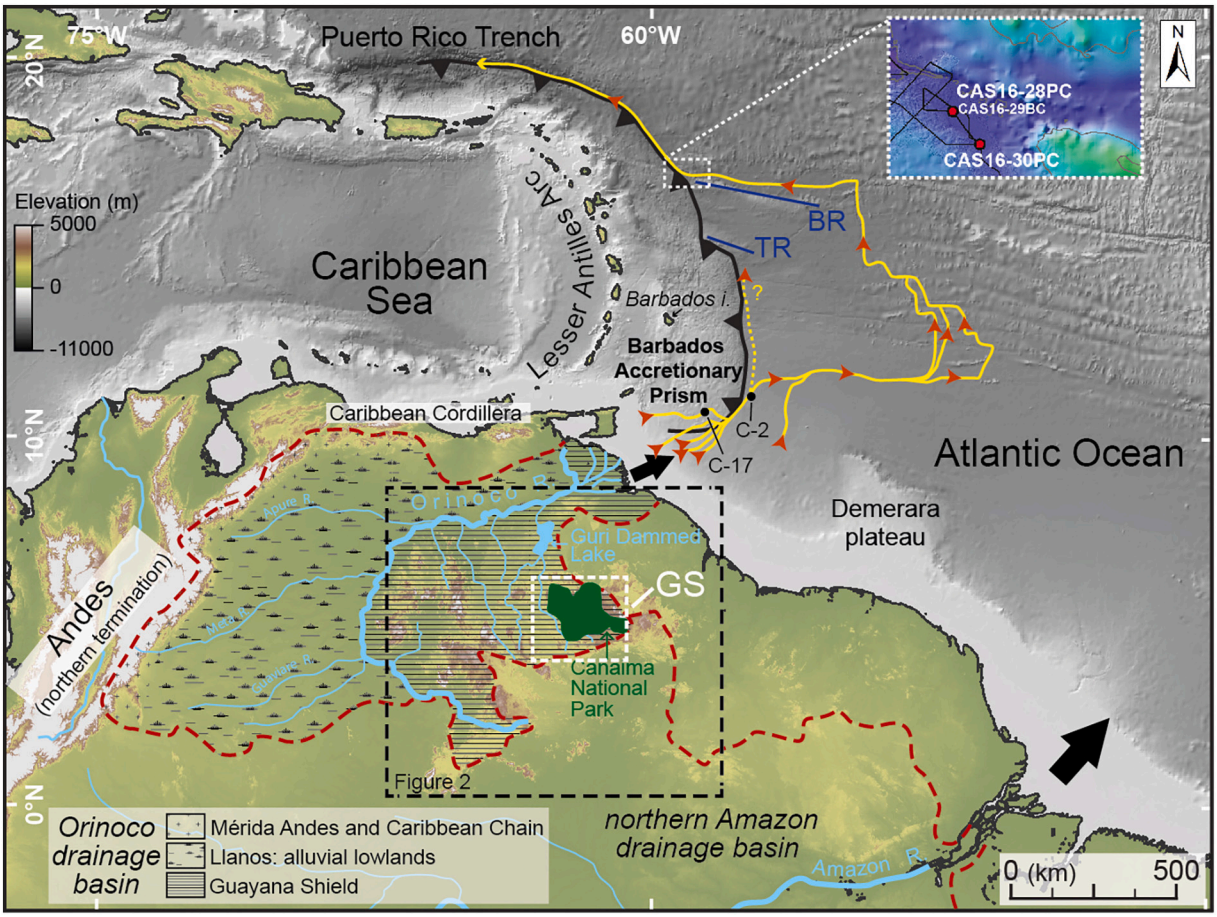

Fig. 1. From the Guyana Shield to the Puerto Rico Trench. Location of the coring sites: red dots of this study, black dots from Deville et al. (2015). Trajectories of oceanic bottom fluxes from the Orinoco Delta following Deville et al. (2015): yellow line with red tringles. Barbados Prism's accretion deformation front: black line with triangles. R.: river; i.: island; TR: Tiburon ridge; BR: Baracuda Ridge; GS: Gran Sabana. (For interpretation of the references to colour in this figure legend, the reader is referred to the web version of this article.)

deepest circulation follows the deformation front of the prism and locally the foot of the Barracuda ridge (Fig. 1). Beside detailed studies of channel-levees systems and turbidites trajectories, Deville et al. (2015) clearly identified active bottom sediments circulation between the Orinoco River mouth and the Atlantic Abyssal floor.

2.2. Guyana shield

Before reaching the Orinoco delta the sediments are eroded and transported via main rivers flowing in the large Orinoco drainage basin. The drainage basin of the Orinoco River can be divided into three zones (Fig. 1), both from morphological and hydrological points of view (de León and Rodríguez Díaz, 1976). Two are mountainous: the eastern slope of the Mérida Andes (from ~5000 m down to ~200 m) and the Guyana Shield (~300 m up to ~2870 m for the highest Roraima plateaux). Between these two highs, lies most of the wide "llanos" alluvial plain which is ~50 to ~100 m above sea-level. This plain is considered to be a zone of dominant accumulation of terrigenous material from the northwest. The Guyana Shield is part of the drainage basin and is a higher relief limited by the Orinoco River (Fig. 1). The mineral fraction contribution to the Orinoco delta is thus mainly issued from the erosion of Archean and Proterozoic rocks: granitic and high-grade metamorphic rocks associated to Tonalite-Trondhjemite-Granodiorite complexes and green belts (1 to 6 on Fig. 2).

Apart from the Roraima orthoquartzitic plateau's isolated remnants, the Guyana Shield displays two different landscapes: rainforest and savannah (respectively A and B, Fig. 3). The savannah ("sabana" in local language) extends almost in the whole south-eastern part of the Guyana Shield, an area locally named "Gran Sabana" (location on Figs. 1 and 2). Although a large part of the Gran Sabana belongs to the Venezuelan Canaima National Park (green on Fig. 1), the Gran Sabana-type landscape can be observed in a larger area (18,000 km^2 surface; within GS-noted square on Figs. 1 and 2; Montoya et al., 2011a and Montoya et al., 2011b). The juxtaposition, in the same morphological and climatic conditions, and on the same geological substratum, led different investigators to analyse the possible origins of this contrast.

The ages of charcoal are coeval with the occurrence of drought in the younger Dryas (Peterson and Haug, 2004) which was followed by an increase of precipitations during the Holocene. This is in agreement with the timing for the alternation of wet and dry periods in the northern part of the South-American continent (Bradley and Diaz, 2021a). The wood fires in Gran Sabana were thus likely promoted because this area underwent a severe drought. The erosion of the Guyana Shield and the transport of the sediment in deep ocean are modulated by climate changes. From a multi-proxy data compilation of the Cariaco Basin, Brazil and Andean sites in Peru, Bolivia, and Ecuador, Bradley and Diaz (2021a) identified three THE in northern part of the south American continent over the last 35 kyr BP: 31 to 30 kyr BP (THE 1), 26 to 23.5 kyr BP (THE 2) and between 18 and 15 kyr BP (THE1). Another rainfall maxima with minor relative amplitude was identified at 12.5 kyr BP.

3. Data and methods

The CASEIS cruise (May/July 2016, Feuillet, 2016) on board R/V POURQUOI PAS? aimed to detect and to decipher the sedimentary imprints of intra-arc vs. giant subduction earthquakes (cf. Feuillet et al., 2011; Seibert et al., 2024), following methodologies previously applied to worldwide subductions (e.g. Goldfinger, 2011). During this cruise, the northern half of the Lesser Antilles forearc, including the Barbados Accretionary Prism, was surveyed with geophysical imaging, giant piston coring (PC) (up to 28 m long), and box-coring (BC). The work presented here concerns cores (Fig. 1 insert), retrieved at the western termination of the Barracuda Rise, more precisely at the junction between the Barracuda Trench and the eastern entrance of the Puerto Rico Trench. We studied two piston cores sampled with a CALYPSO giant Küllenberg-type coring system: CAS16-28PC and CAS16-30PC (sites coordinates and depths below seafloor on Fig. 4). The sampling site of core CAS16-28PC was complemented by the interface core CAS16-29BC using a box-corer system.

Five samples of organic matter and charcoal from core CAS16-28PC have been processed for ^{14}C AMS dating, two at Poznan Radiocarbon Laboratory, and three at CNRS LMC14 Laboratory in Saclay (Table 1). The radiocarbon ages were calibrated using OxCal 4.4 software (Bronk Ramsey, 2009) with intcal20.14c calibration curve (Reimer et al., 2020). Grain size analyses were performed on core CAS16-29BC using a laser diffraction microgranulometer MALVERN™ Mastersizer 2000 at ISTerre Laboratory, Savoie-Mont-Blanc University. This equipment has a 0.02 to 2000 μm range. Smear slides were sampled throughout the cores and

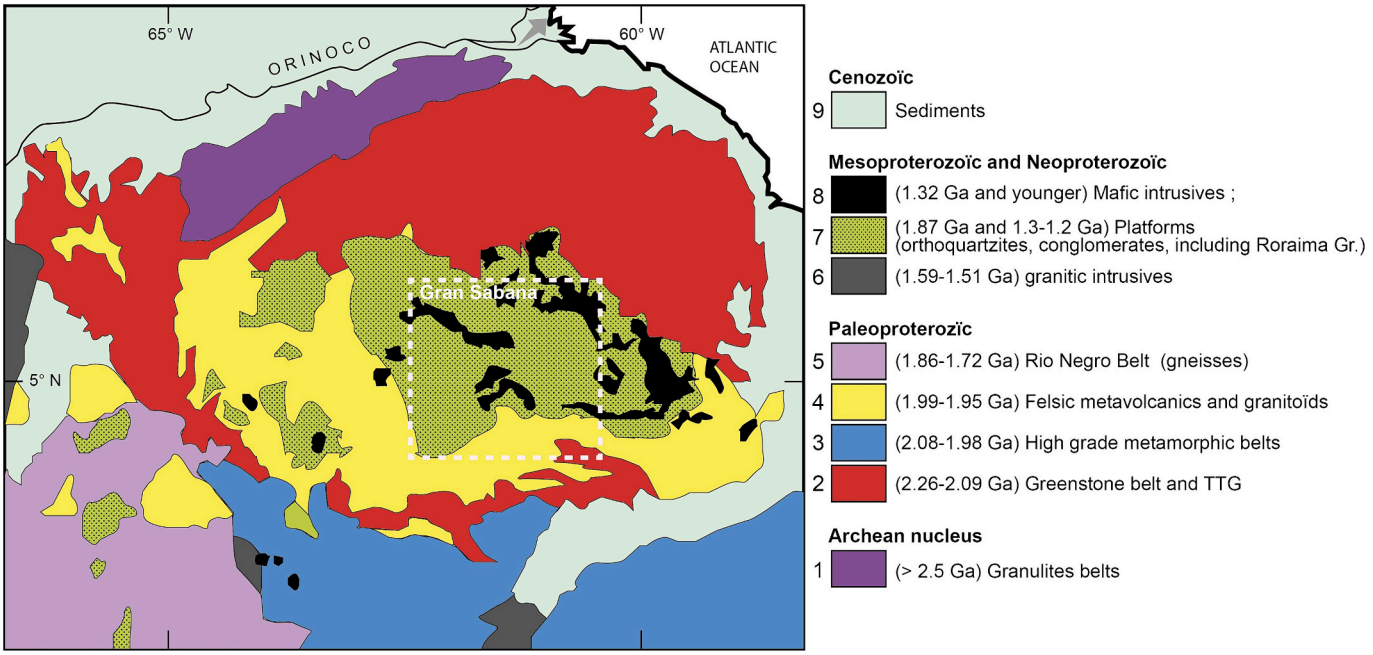

Fig. 2. Simplified geological map of northern Guyana Shield, adapted from Kroonenberg et al. (2016). Location on Fig. 1. Dotted white square: Gran Sabana.

Fig. 3. Landscapes views of the Guyana Shield between Orinoco River and northern Brasil frontier. A: rainforest within the Canaima National Park; B: Gran Sabana landscape, with patches of "moriche"-type palm tree (*Mauritius flexuosus*). Horizontal tabular relieves correspond to the Neo-Proterozoic Roraima Group.

observed under binocular and microscope. Moreover, HCl tests on the sediment were performed to characterize the carbonate content.

More analyses were made on the non-organic fraction. It was mechanically separated (no chemical treatment) and the silt-fine sand fraction was mounted within epoxy and analysed as a polished uncovered thin section. The X-Ray element distribution maps and quantitative point analyses were performed on JEOL JXA-8230 electron probe microanalyser (EPMA) at the Institut des Sciences de la Terre (ISTerre), Grenoble Alpes University, (e.g. Batanova et al., 2018). The data acquisition was made in wavelength dispersive spectrometry mode (WDS). We used a 15 kV accelerating voltage, and a 12 nA probe current for X-ray-mapping and spot analyses. The beam with diameter 5 μm was used to avoid surface damage of soft minerals. The standardisation was made using certified natural minerals and synthetic oxides. The ZAF correction procedure was applied. For X-ray maps, the beam was focused (spot), the step (pixel) size was 1 μm and well time 50 msec per pixel.

4. Results

4.1. Lithostratigraphy

Surprisingly, CAS16-28PC and CAS16-30PC coring attempts failed in the trench as the corer could not penetrate more than 1.2 m (Fig. 4), while we were able to sample up to 29 m long cores in neighbouring intra-wedge and fore arc basins (Seibert et al., 2024). At least 60 cm of a mixture of vegetal debris, charcoal, and silty clay prevented more penetration (core CAS16-28PC).

Core CAS16-28PC contains, from base to top (Fig. 4): 1) few centimetres of dark grey organic-rich fine-grained mud, 2) mixture of coarse organic vegetal fragments and siliciclastic silt/very fine sand, 3) structure-less non calcareous clayey silt. Core CAS16-30PC yielded laminated light brown non calcareous mud slightly disturbed by coring (Fig. 4). Similar laminated levels appeared in box core CAS16-29BC. Laminae are 1 to 5 mm thick, grading from a darker base to a light brown upper part. Laser grain-size was performed on the 19 to 48 cm depth in core interval, in CAS16-29BC. The following results were obtained: 3.8 to 8.2 μm D50; 6 to 8 μm mode (Supplementary material 1). All particles thus belong to clay and silt size. Measurements do not display significant difference within each individual layer.

4.2. The Baracuda Trench organic debrite

We focused our analyses on Core CAS16-28PC. Apart from a high organic content, it also presents a mineral fraction mainly made of white mica. Despite slight coring disturbance, the top of the deposit appears rather neat but irregular. Its base was not reached, and within the sampled part, we did not observe any clear layering which could have represented a classical turbidite sequence. However, we can't totally exclude this hypothesis because of the texture change highlight on the photo of the core from the bottom to the top of the deposit (Fig. 4). Fig. 5 illustrates the heterogeneity of its content. Due to its "allochtonous" transported content, we consider this layer as an "event deposit" and

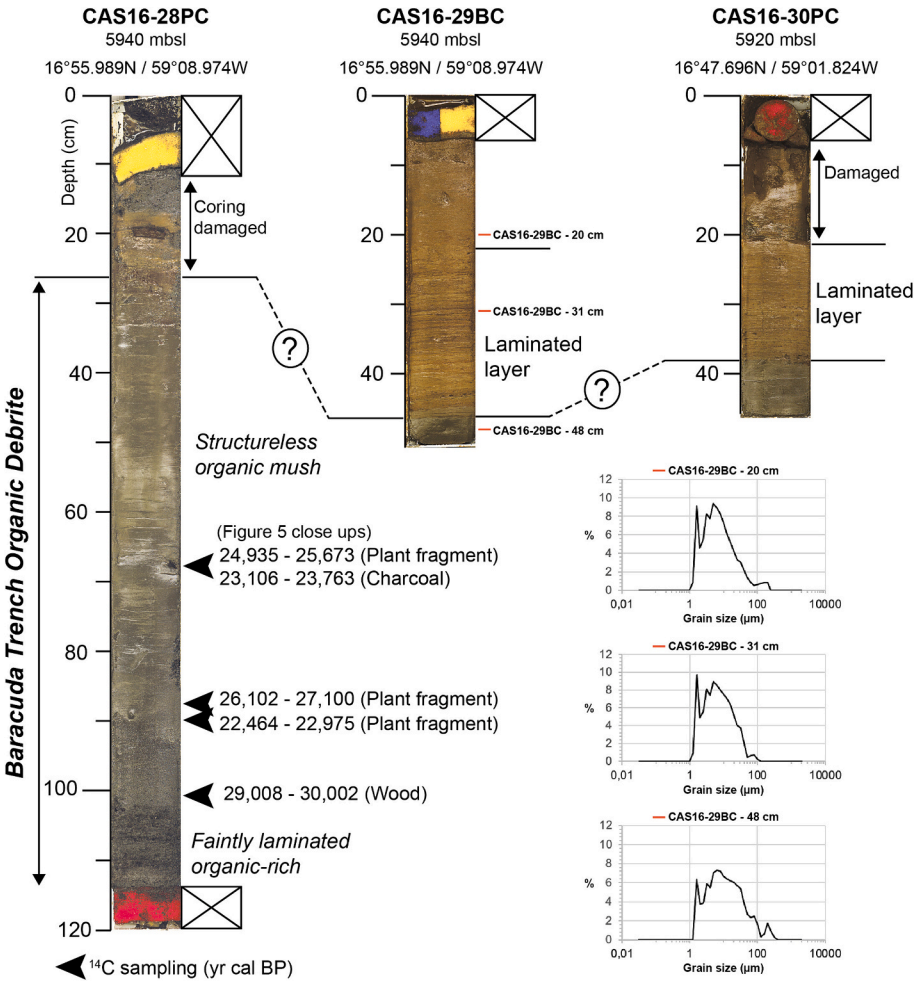

Fig. 4. The CAS16-28PC, CAS16-29BC, and CAS16-30PC cores: view of split cores and simplified lithostratigraphy. Indicated coordinates correspond to the vessel position.

Table 1
14C dating results.

Sample	Material	Radiocarbon Age BP	Calibrated age - yr BP- 2	Analyst
CAS16-28PC 68/67 cm - A	plant fragment	20,940 +/- 140	24,935 – 25,673	Radocarbon Lab. Poznan
CAS16-28PC 68/67 cm - B	charcoal	19,440 +/- 110	23,106 – 23,763	Radocarbon Lab. Poznan
CAS16-28PC 87/88 cm	plant fragment	22,310 +/- 170	26,102 – 27,100	Saclay CNRS ARTEMIS
CAS16-28PC 89/90 cm	plant fragment	18,820 +/- 120	22,464 – 22,975	Saclay CNRS ARTEMIS
CAS16-28PC 100/ 101 cm	wood	25,180 +/- 240	29,008 – 30,002 (*) intcal20.14c, Reimer et al., 2020	Saclay CNRS ARTEMIS

named it a “debrite”, avoiding a genetic term, and as proposed for similar deposits (Huyghe et al., 2004; Deville et al., 2006; Callec et al., 2010). We name this particular layer “Barracuda Trench” (BT) organic debrite with respect to its discovery location at the Barracuda Trench-Puerto Rico Trench junction.

4.2.1. Organic content and ^{14}C dating

Close-ups a to d of Fig. 5 illustrate the dominance of vegetal organic matter (O.M.): leaves and wood fragments, and seeds. Close up c shows charcoal (black) surrounding a seed (light brown). The size of unburned wood fragments and charcoal particles may reach up to 1 cm. Five radiocarbon ages were obtained from plant, wood, and charcoal samples, from CAS16-28PC (Table 1). Calibrated ages of plant fragments range between 22,460 and 27,100 yr. BP. The wood fragment appears slightly older, between 29,000 and 30,000 yr. BP. The analysed charcoal sample ranges from 23,100 to 23,760 yr BP. The five measured ages belong to Late Pleistocene. With respect to global Quaternary paleoclimatic scale, they all belong to Marine Isotopic Stages (MIS) 2 and the end of the MIS 3 interval.

4.2.2. Mineral content

Preliminary binocular observations pointed out abundant silt-size white mica crystals. Microscopic observations (Fig. 5, close-ups e to g) display other minerals: calcite, microcline, sphene (titanite), and corroded quartz. In order to confirm and refine these observations, microprobe analyses were performed (Table 2). The occurrence of microcline, sphene (titanite), and muscovite is confirmed; K-Na feldspar

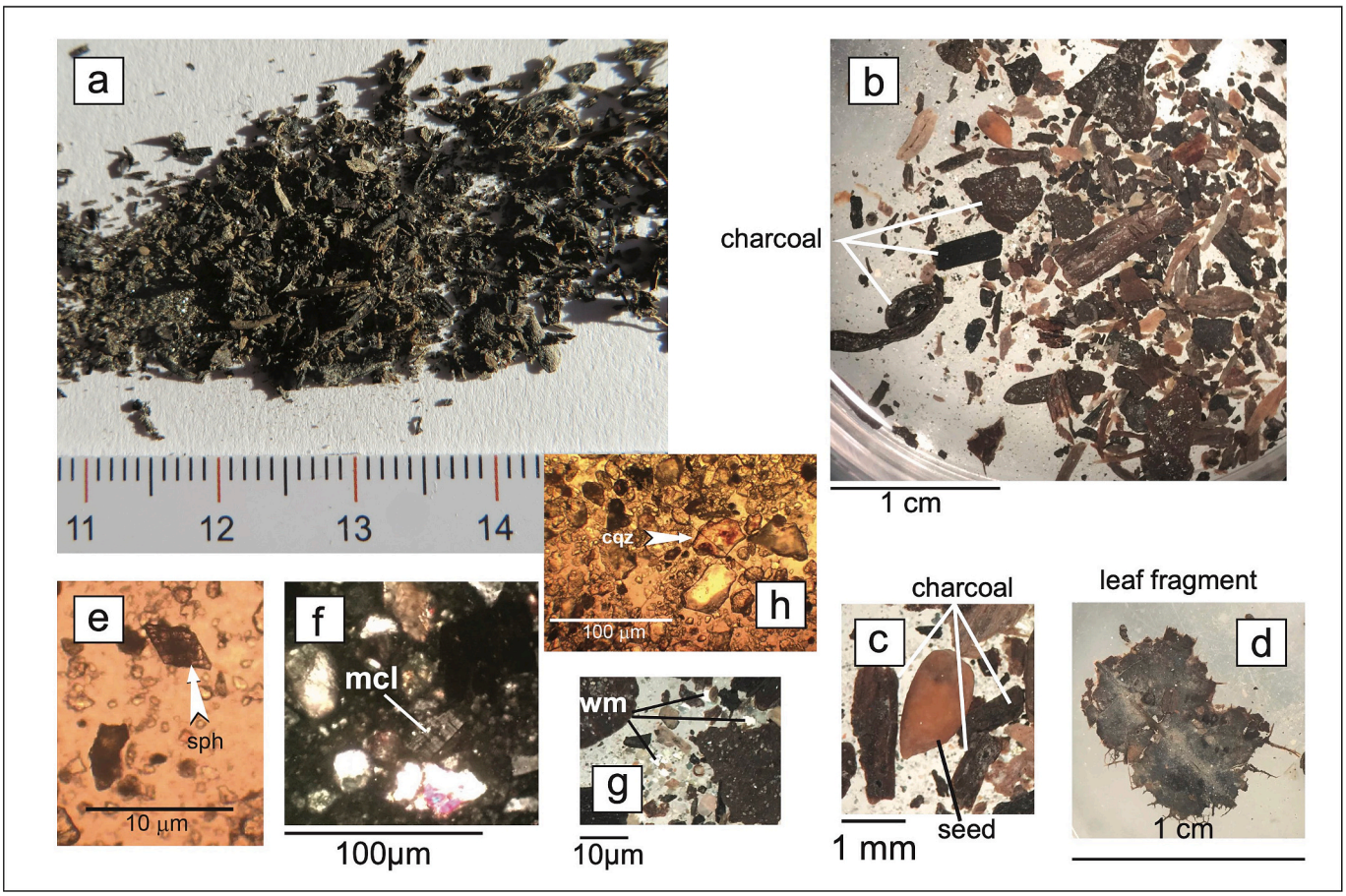

Fig. 5. Close up of organic-rich level content (organic and siliciclastic) from the core CAS16-28PC (location on Fig. 4). a to d: binocular views (a: raw spatula sample; b to c, after water cleaning and dispersion); e to h: microscope views (f and g: polarized light). Sph: sphenen (titanite); mcl: microcline; cqz: corroded quartz; wm: white micas.

(crypto-perthites) and albite, ilmenite, rutile, and low-Ti magnetite, were also identified. The whole set of silicates indicates a continental igneous-metamorphic (granitic, gneissic) origin. The composition of calcite crystal fragments, in addition to their microscopic aspect, suggests either marble fragments or secondary calcite in metamorphosed igneous or volcanic rocks.

5. Discussion: Origin of BT organic debrite content, possible paleo-climatic implications

5.1. Depositional processes

The results of the two piston coring sites (CAS16-28PC and -30PC) and the associated box coring site (CAS16-29BC) are summarised in Fig. 4. The upper part of a highly organic and siliclastic level responsible for the reduced corer penetration is present in the three cores. We attribute the difference between cores CAS16-28PC and CAS16-29BC (taken with the same vessel position) to the coring techniques. The difference between cores CAS16-28PC and CAS16-30PC (occurrence vs. lack of laminated interval) may also be explained by a higher coring disturbance for the core CAS16-28PC. Such difference between the piston cores of the CASEIS cruise has also been showed by Seibert et al. (2024). We propose a correlation between the upper part of the above-named "BT debrite" (in CAS16-28PC) and the lower part reached in cores CAS16-29BC and CAS16-30PC. The three levels possibly represent the same layer, but even in the thickest section (Core CAS16-28PC), its base was not reached. The mineral fractions of the BT debrite does not match a provenance from the nearest aerial vegetation of the neighbouring Lesser Antilles islands, implying an alternative, more distant source.

We did not observe any neat internal layering characteristic of a lateral bottom transportation, as a turbiditic process, only the lowest 10 cm in Core CAS16-28PC display a faint layering. The BT debrite differs from a classical terrigenous turbidite involving a unique depositional event over a large distance along a simple trajectory (e.g. Elmore et al., 1979), and we may not discard the interpretation of this conspicuous layer as a complex polyphase event.

Previous investigations dedicated to the Barbados Prism (CARAMBA cruise; Callec et al., 2010; Deville et al., 2015) complement our interpretations, both for the BT debrite (Core CAS16-28PC) and for the overlying laminated sediments (Cores CAS16-29BC and CAS16-30PC). Core CAS16-28PC lithostratigraphic pattern is similar to CARAMBA Core C-2 succession (~2.5 m-long). Core C-2 was also retrieved in the trench corresponding to the deformation front, but in the southern part of the Barbados Prism at a 4282 m water depth, in a targeted channel overbank situation (location on Fig. 1). There, the basal part of a similar organic debrite did not display specific layering. CARAMBA Core C-17 (Huyghe et al., 2004; Deville et al., 2006; Callec et al., 2010; location on Fig. 1), taken in levee position displayed laminated sediments; we follow the same interpretation (channel-levee deposit) for our observed laminated sediments, upper part of the core CAS16-29BC and -30PC. The BT debrite could represent a particularly strong bottom flowing (single vs. polyphasic?) event.

Table 2
Microprobe analysis of the siliciclastic and carbonate fractions (separate clasts) from organic-rich level within Core CAS16-28PC.

SiO2	TiO2	Al2O3	FeO	MnO	MgO	CaO	Na2O	K2O	Cr2O3	NiO	Cl	Total	
65.12	0.00	17.64	0.08	0.00	0.00	0.03	0.28	15.89	0.00	0.00	0.00	99.05	microcline
66.47	0.00	18.28	0.06	0.00	0.00	0.03	0.24	16.22	0.00	0.00	0.00	101.32	microcline
67.19	0.00	18.48	0.07	0.00	0.00	0.03	0.47	15.72	0.02	0.02	0.01	102.00	microcline
63.70	0.03	18.09	0.04	0.00	0.01	0.06	0.29	16.04	0.00	0.00	0.01	98.28	microcline
64.59	0.01	17.44	0.07	0.00	0.00	0.11	0.49	15.38	0.00	0.03	0.00	98.11	microcline
64.49	0.01	19.04	0.07	0.01	0.00	0.03	0.22	16.31	0.01	0.00	0.00	100.20	microcline
66.74	0.00	18.97	0.03	0.00	0.00	0.09	11.49	0.05	0.00	0.00	0.00	97.38	albite
73.08	0.01	19.73	0.10	0.00	0.01	0.07	13.47	0.03	0.00	0.00	0.00	106.50	albite
65.60	0.01	18.83	0.21	0.00	0.00	0.09	11.12	0.07	0.00	0.03	0.00	95.96	albite
68.66	0.01	20.09	0.14	0.01	0.10	0.43	12.16	0.15	0.00	0.03	0.00	101.78	albite
68.26	0.00	21.19	0.13	0.01	0.00	1.05	11.82	0.14	0.00	0.00	0.01	102.60	albite
68.24	0.00	18.51	0.48	0.00	0.00	0.11	11.76	0.15	0.00	0.00	0.01	99.28	albite
69.56	0.00	18.30	0.07	0.00	0.01	0.11	12.51	0.09	0.01	0.03	0.00	100.69	albite
67.55	0.01	19.57	0.45	0.03	0.02	1.50	11.41	0.39	0.00	0.05	0.01	100.98	albite
70.65	0.00	20.46	0.04	0.00	0.00	0.08	10.17	0.03	0.00	0.00	0.00	101.43	albite
65.40	0.02	18.72	0.18	0.00	0.01	0.06	6.60	7.47	0.00	0.02	0.02	98.50	K-Na feldspar cryptoperthites
66.82	0.00	18.93	0.03	0.02	0.00	0.14	5.93	7.62	0.00	0.00	0.00	99.49	K-Na feldspar cryptoperthites
49.07	0.38	29.82	2.11	0.01	1.97	0.08	0.50	9.78	0.03	0.00	0.00	93.75	muscovite
0.54	92.31	0.30	1.00	0.00	0.00	0.40	0.00	0.03	0.04	0.00	0.01	94.63	rutile
28.59	36.96	1.19	0.80	0.07	0.00	28.53	0.00	0.01	0.00	0.00	0.00	96.15	sphene/titanite
29.38	34.12	2.63	1.64	0.09	0.00	28.11	0.00	0.01	0.00	0.00	0.00	95.99	sphene/titanite
0.85	3.54	0.09	81.47	0.09	0.00	0.19	0.00	0.04	0.00	0.06	0.02	86.36	low-Ti magnetite
0.35	48.43	0.54	36.25	2.57	0.05	0.86	0.04	0.01	0.12	0.00	0.02	89.24	ilmenite
MgO	CaO	FeO	MnO	SrO	BaO	CO2	Total						
0.00	58.37	0.08	0.04	0.01	0.00	41.49	100.00	calcite					
0.16	56.45	0.12	0.00	0.00	0.03	43.24	100.00	calcite					
0.09	56.54	0.25	0.01	0.00	0.00	43.10	100.00	calcite					
0.21	51.63	0.35	0.06	0.00	0.06	47.70	100.00	calcite					
0.23	55.48	0.46	0.15	0.00	0.04	43.64	100.00	calcite					
0.07	54.01	0.30	0.03	0.00	0.02	45.57	100.00	calcite					
0.33	54.79	0.63	0.06	0.11	0.00	44.09	100.00	calcite					
0.07	56.59	0.12	0.02	0.01	0.00	43.18	100.00	calcite					
0.01	58.02	0.08	0.04	0.00	0.05	41.80	100.00	calcite					

5.2. Origin and pathway of the BT debrite's reworked material

This oceanic bottom circulation depicted by Deville et al. (2015) is directly fed by the Orinoco River feeding through its delta. In addition, the Demerara Plateau (Fig. 1) prevents bottom circulation coming from East/South-East, in particular from the Amazon delta and from the Antarctic Bottom Water (AABW). The interpreted continental provenance of the organic fraction is in agreement with pyrolysis performed by Deville et al. (2015) on organic levels from cores taken in the frontal part of the Barbados Prism; their results indicated terrestrial vegetal origin (Type III Organic Matter). Our results concerning the non-organic fraction from Core CAS16-28PC indicate erosion products of continental lithosphere; corroded quartz grains indicate tropical humid alteration (Fig. 5h). A provenance of the BT debrite from the Guyana Shield is thus proposed. Cores CARAMBA C-2 and CAS16-28PC should represent two coring sites on the same main depositional trajectory (Fig. 1).

5.3. Age and link with a specific climatic period

The occurrence of charcoal and the morphological/hydrological relationships between the Orinoco River and the Guyana Shield, lead us to discuss links between this particular sedimentary content and drastic vegetation changes on the Guyana Shield, more precisely in the Gran Sabana area. Severe drought, abruptly following wet periods with abundant vegetation, represent favorable conditions for large wood fires.

The period of interest is between ~30 and ~ 23 kyr BP, taking into account the calibrated maximum and minimum measured ages, including charcoal age (Fig. 6). Given the sedimentation rate of 1.32 cm/kyr obtained near the location of this study-core (from the Leg 110, Mascle et al., 1988) and the most recent rate of 1.67 cm/kyr obtained from a sediment core sampled on a high relief of the Barbados accretionary prism (Bieber et al., 2021), and considering the 40 cm of

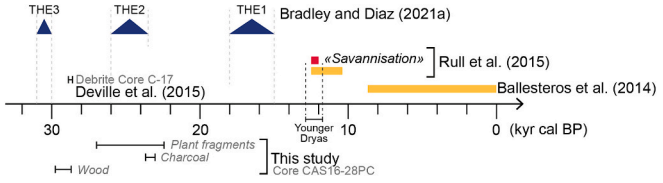

Fig. 6. Simplified chronological position of the BT debrite data, with respect to regional paleoclimatic data. Orange bar: occurrence of particulate charcoal in lacustrine deposits.

sediment above the BT debrite, we calculated an approximate age of between 30.8 and 23.9 kyr. We have to mention a 24,480 ± 140 yr. uncalibrated ^{14}C age obtained by Deville et al. (2015), 28,740 ± 180 yr cal BP, on O.M. from an organic debrite intercalated within levee deposit bounding a now inactive canyon. For this period, according to the above-mentioned paleo-climatic data (Bradley and Diaz, 2021a), vegetation could develop on Guyana Shield with THEs 2 and 3. Dry period, maybe associated to severe droughts, likely alternated with these THE wet periods between 28 and 27 kyr BP, 23 and 18 kyr BP, and 14 and 13 kyr BP (Fig. 6). Wood fires indicated by the charcoal fragments contained in Core CAS16-28PC may have occurred after THE2. Based on pollen records in different sites in the south of the study area, Salgado-Labouriau (1997) and Salgado-Labouriau et al. (1997) mention treeless grassland between 32 and 20 kyr BP due to humid conditions. However, these authors attribute a lack of actual forest to coeval low temperature. Regarding the chronology, the BT debrite's vegetal remnants appear included within this time interval, but they are mainly coming from trees. This difference may be explained by the more southern location of the sites analysed by these authors. For the last 15 kyr, the data directly concerning the Gran Sabana (Montoya et al., 2011a and b; Ballesteros et al., 2014; Rull et al., 2015) mention rainforest till ~12 kyr BP.

Concerning charcoal occurrence within core CAS16-28PC, we may

refer either to: i) the mention of "charcoal before 20 kyr BP" by Salgado-Labouriau (1997) and Salgado-Labouriau et al. (1997), or ii) the hypothesis of an interval THE2-THE1 favorable for wood fires occurrences. In both cases, we have to consider the here-evidenced rainforest-to-savannah change as predating that characterized by Montoya et al. (2011a and b), Ballesteros et al. (2014), and Rull et al. (2015). This older event may be synchronous with MIS3-to-MIS2 transition, but we lack data on a potential local record in the Gran Sabana itself. An alternative hypothesis would be that we did not record the last Gran Sabana evolution in our cores.

From a sedimentary point of view, the mobilization of wood fire products (including no burned fragments), together with mineral fraction, can result from rainy episodes (immediately?) following the consequence of drought. The very large distance between the Guyana Shield and the Puerto Rico trench leads to the question of the age of this transport and subsequent deposition: 1) is the BT organic debrite associated either with a unique reworking event or with a short interval with few successive reworking events?, 2) did the distant re-deposition occur shortly after wood-fire denudation or was there a delay between both? Based on our dataset, no internal structures within the BT layer was observed. Thus, we could not decipher monophasic vs. polyphasic deposition. According to its fine grain-size, the non-organic fraction clearly represents a potential suspended load, transported by actual turbiditic as well as contouritic processes. We suggest that the organic remnants and charcoal may have been mobilized soon after their genesis through a rapid rainfall increase (THE), their ^{14}C age might represent a rough estimate for the age of the debrite deposition.

6. Conclusions

The particular organic-siliciclastic layer found at the south-eastern entrance of the Puerto Rico Trench (Core CAS16-28PC) represents an entirely "allochtonous" set of terrestrial vegetal and mineral remnants issued from the Guyana Shield. Its occurrence confirms the Late Pleistocene continuation of the South-American terrigenous feeding of the Barbados Accretionary Prism. The present-day location of this material confirms the long and complex bottom circulation pattern connecting the Orinoco River mouth and the Puerto Rico Trench, as defined by Deville et al. (2015). The exceptionally long path (> 2000 km for the oceanic part) implies probable relays of actual density currents and contouritic effects.

We infer that the vegetal remnants and the abundant charcoal contained in the Barracuda Trench organic debrite represent remote evidence for an abrupt climatic change (rainy conditions to severe drought) which affected the Guyana Shield. Based on the obtained ages of the organic material (between ~30 and ~ 23 kyr BP) this change may have occurred at MIS3-MIS2 transition. This also could correspond to the interval between Tropical Hydrological Events 2 and 1 defined by Bradley and Diaz (2021a). According to direct (local) paleo-climatic data (Montoya et al., 2011a and b; Ballesteros et al., 2014; Rull et al., 2015), the involved area - called the Gran Sabana - underwent such an abrupt change during the Younger Dryas, much more recent than that documented here. Our results suggest older wood fire events and thus re-evaluate the age of the "Gran Sabana". The complex tectonic and sedimentary evolution of the Barbados Prism may have trapped and preserved evidence for older climatic events undergone by Northern South-America. As a corollary, we suggest that the incorporation of the corresponding organic levels within the accreted pile, by mean of off-scraping, may include such terrestrial material. We may wonder if the thermogenic methane detected both at the deformation front (cold seepage and specific fauna) and along active thrusts (ODP Leg 110 Scientific Party, 1987; Blanc et al., 1988; Moore et al., 1988) is at least partly related to the transformation of this organic matter.

CRediT authorship contribution statement

Chloé Seibert: Writing – review & editing, Writing – original draft, Visualization, Validation, Methodology, Investigation, Formal analysis. **Christian Beck:** Writing – review & editing, Writing – original draft, Visualization, Validation, Resources, Methodology, Investigation, Formal analysis, Conceptualization. **Nathalie Feuillet:** Writing – review & editing, Visualization, Validation, Resources, Project administration, Investigation, Funding acquisition, Formal analysis. **Eva Moreno:** Writing – review & editing, Visualization, Validation, Resources, Investigation, Formal analysis, Data curation. **Denise Pons:** Visualization, Validation, Investigation, Formal analysis. **Chris Goldfinger:** Writing – review & editing, Visualization, Validation, Investigation, Formal analysis, Conceptualization. **Gueorgui Ratzov:** Writing – review & editing, Visualization, Validation, Investigation, Formal analysis. **Guillaume St-Onge:** Writing – review & editing, Visualization, Validation, Investigation, Formal analysis. **Arthur Bieber:** Visualization, Validation, Investigation, Formal analysis. **Pierre Morena:** Visualization, Validation, Investigation, Formal analysis. **Jason Patton:** Visualization, Validation, Investigation, Formal analysis. **Valentina Batanova:** Visualization, Validation, Methodology, Investigation, Formal analysis. **René Maury:** Writing – review & editing, Visualization, Validation, Investigation, Formal analysis.

Declaration of competing interest

We do not have conflicts of interest to report.

Data availability

Data will be made available on request.

Acknowledgements

The CASEIS Cruise and further associated laboratory investigations were supported by CARQUAKES Grant funded by French Agence Nationale de la Recherche (ANR-17-CE03-0006). Part of the AMS ^{14}C measurements were conducted through ARTEMIS facility procedure developed and funded by the Centre National de la Recherche Scientifique (CNRS). We acknowledge Pierre Sabatier and Fayçal Soufi (EDYTEM Laboratory, Savoie-Mont-Blanc University) respectively for advising the calibration of ^{14}C ages, and for the preparation of the samples for microprobe analysis. All the collected cores during the CASEIS Cruise are stores in the marine collection of the National Museum of Natural History, France, and have the prefix MNHN-GS (https://science.mnhn.fr). Thanks to the anonymous reviewer and associate editor for their constructive comments that helped to improve the clarity of the manuscript.

Appendix A. Supplementary data

Supplementary data to this article can be found online at https://doi.org/10.1016/j.palaeo.2024.112497.

References

Ballesteros, T., Montoya, E., Vegas-Vilarrúbia, T., Giralt, S., Abbott, M.T., Rull, V., 2014. An 8700-year record of the interplay of environmental and human drivers in the development of the southern Gran Sabana landscape, SE Venezuela. The Holocene 24 (12), 1757–1770.

Batanova, V.G., Sobolev, A.V., Magnin, V., 2018. Trace element analysis by EPMA in geosciences: detection limit, accuracy and precision. IOP Conf. Ser. Mater. Sci. Eng. 304 (1), 012001. https://doi.org/10.1088/1757-899X/304/1/012001.

Beck, C., Ogawa, Y., Dolan, J., 1990. Eocene paleogeography of the southeastern Caribbean: relations between sedimentation on the Atlantic Abyssal Plain at Site 672 and evolution of the South-America margin. In: Moore, J.C., Mascle, A., et al. (Eds.), Proceedings of the Ocean Drilling Program, Scientific Results, 110, pp. 7–15.

Bénâtre, G., Feuillet, N., Carton, H.D., Pichot, T., Jacques, E., Deplus, C., Leclerc, F., 2022, December. Forearc strain partitioning in the Martinique-Antigua sector of the lesser antilles subduction zone. In: AGU Fall Meeting Abstracts, 2022. T53B-06.
Bieber, A., St-Onge, G., Feuillet, N., Carlut, J., Moreno, E., Michel, E., 2021. Regional chronostratigraphy in the eastern Lesser Antilles quaternary fore-arc and accretionary wedge sediments: Relative paleointensity, oxygen isotopes and reversals. Quat. Geochronol. 65, 101179.
Biju-Duval, B., Le Quellec, P., Renard, V., Mascle, A., Valéry, P., 1982. Multibeam bathymetric survey and high resolution seismic investigations on the Barbados Ridge complex (Eastern Caribbean): a key to the knowledge and interpretation of an accretionary wedge. Tectonophysics 86 (1–2), 275–304.
Blanc, G.É., Gieskes, J.M., Vrolijk, P.J., Mascle, A.L., Moore, C.J., Taylor, E.L., Alvarez, F., Andreieff, P.A., Barnes, R., Beck, C., Behrmann, J., 1988 May 1. 1988. Advection de fluides interstitiels dans les series sédimentaires du complexe d'accretion de la Barbade (Leg 110 ODP). Bulletin de la Société géologique de France. 4 (3), 453–460.
Bradley, R.S., Diaz, H.F., 2021a. Late quaternary abrupt climate change in the tropics and sub-tropics: the continental signal of tropical hydroclimatic events (THEs). Rev. Geophys. 59, e2020RG000732.
Bradley, R.S., Diaz, H.F., 2021b. Understanding abrupt climate change in the late quaternary. Eos 102. https://doi.org/10.1029/2021EO215005.
Bronk Ramsey, C., 2009. Bayesian analysis of radiocarbon dates. Radiocarbon 51 (1), 337–360. https://doi.org/10.1017/s0033822200033865.
Callec, Y., Deville, E., Desaubliaux, G., Griboulard, R., Huyghe, P., Mascle, A., Mascle, G., Noble, M., Padrón de Carillo, C., Schmitz, J., 2010. The Orinoco turbidite system: Tectonic controls on sea-floor morphology and sedimentation. Am. Assoc. Pet. Geol. Bull. 94 (6), 869–887.
Capet, X., Chamley, H., Beck, C., Holtzapffel, T., 1990. Clay mineralogy of sites 671 and 672, Barbados Ridge accretionary complex and Atlantic Abyssal Plain: paleoenvironmental implications. In: Moore, J.C., Mascle, A., et al. (Eds.), 1990 Proceedings of the Ocean Drilling Program, Scientific Results, 110, pp. 85–96.
de Carrillo, C.P., 2007. Les interactions tectonique et sédimentation entre le front du prisme de la Barbade et le derlat de l'Orénoque. In: Doctoral dissertation, Université Joseph-Fourier-Grenoble I.
de León, R., Rodríguez Díaz, A.J., 1976. Mapa de la Cuenca del Orinoco, in "El Orinoco aprovechado y recorrido".
Deville, E., Guerlais, S.H., Callec, Y., Griboulard, R., Huyghe, P., Lallemant, S., Mascle, A., Noble, M., Schmitz, J., Desaubliaux, G., Ellouz, N., Prinzhofer, A., Lebrun, J.F., Mascle, G., Padrón de Carrillo, C., Cana, R., Foucher, J.-P., 2006. Liquefied *vs.* stratified sediment mobilization processes: Insight from the South of the Barbados accretionary prism. Tectonophysics 428, 33–47.
Deville, E., Mascle, A., Callec, Y., Huyghe, P., Lallemant, S., Lerat, O., Mathieu, X., Padrón de Carillo, C., Patriat, M., Pichot, T., Loubrieux, B., Granjeon, D., 2015. Tectonics and sedimentation interactions in the East Caribbean subduction zone: an overview from the Orinoco delta and the Barbados accretionary prism. Mar. Pet. Geol. 64, 76–103.
Dolan, J., Beck, C., Ogawa, Y., 1989. Upslope deposition of extremely distal turbidites: an example from the Tiburon rise, west-Central Atlantic. Geology 17, 990–994.
Elmore, R.D., Pilkey, O.H., Cleary, W.J., Allen Curran, H., 1979. Black Shell turbidite, Hatteras Abyssal Plain, western Atlantic Ocean. Geol. Soc. Am. Bull. 90, 1165–1176.
Feuillet, N., 2016. CASEIS cruise, RV Pourquoi pas? https://doi.org/10.17600/16001800.
Feuillet, N., Beauducel, F., Tapponnier, P., 2011. Tectonic context of moderate to large historical earthquakes in the Lesser Antilles and mechanical coupling with volcanoes. J. Geophys. Res.: Solid Earth (1978–2012) 116 (B10).
Goldfinger, C., 2011. Submarine paleoseismology based on turbidite records. Annu. Rev. Mar. Sci. 3, 33–66. https://doi.org/10.1146/annurev-marine-120709-142852.
Haug, G.H., Hughen, K.A., Sigman, D.M., Perterson, L.C., Röth, U., 2001. Southern migration of the intertropical convergence zone through the Holocene. Science 293 (5533), 1304–1308.
Hoffmann, J., Bahr, A., Voigt, S., Schönfeld, J., Nürnberg, D., Rethemeyer, J., 2014. Disentangling abrupt deglacial hydrological changes in northern South America: insolation *versus* oceanic forcing. Geology 42 (7), 579–582.
Huyghe, P., Foata, M., Deville, E., Mascle, G., Cagna, R., Callec, Y., Desaubliaux, G., Ellouz, N., Griboulard, R., Guerlais, S.H., Lallemant, S., Lebrun, F., Mascle, A., Mugnier, J.L., Padrón, C., Prinzhofer, A., Schmitz, J., Wendenbaum, E., Caramba Working Group, 2004. Channel profiles through the active thrust front of the southern Barbados prism. Geology 32, 429–432.
Kroonenberg, S.B., de Roever, E.W.F., Fraga, L.M., Reis, N.J., Faraco, M.T., Lafon, J.M., Cordani, U.G., Wong, T.E., 2016. Paleoproterozoic evolution of the Guiana shield in Suriname: a revised model. Geologie en Mijnbouw, Netherl. J. Geosci. 95, 491–522.
Larue, D.K., Speed, R.L., 1983. Quartzose turbidites of the accretionary complex of Barbados, I: Chalky Mount succession. J. Sediment. Petrol. 53 (4), 1337–1352.
Mascle, A., Moore, J.C., 1990. ODP Leg 110: tectonic and hydrology synthesis. In: Proceedings of the Ocean Drilling Program, Scientific Results, 10, pp. 409–422.
Mascle, A., Moore, J.C., et al., 1988. Proc, Init. Repts. (Pt. A), ODP, 110: College Station, TX (Ocean Drilling Program). Site 672. https://doi.org/10.2973/odp.proc.ir.110.106.1988.
Montoya, E., Rull, V., Stansell, N.D., Abbott, M.B., Nogué, S., Bird, B.W., Díaz, W.A., 2011a. Forest–savanna–morichal dynamics in relation to fire and human occupation in the southern Gran Sabana (SE Venezuela) during the last millennia. Quat. Res. 76, 335–344.
Montoya, E., Rull, V., Stansell, N.D., Bird, B.W., Nogué, S., Vegas-Vilarrùbia, T., Abbott, M.B., Diaz, W.A., 2011b. Vegetation changes in the Neotropical Gran Sabana (Venezuela) around the Younger Dryas Chron. J. Quat. Sci. 25, 207–218.
Moore, J.C., Mascle, A., Taylor, E., Andreieff, P., Alvarez, F., Barnes, R., Beck, C., Behrmann, J., Blanc, G., Brown, K., Clark, M., 1988 Oct 1. Tectonics and hydrogeology of the northern Barbados Ridge: results from Ocean Drilling Program Leg 110. Geol. Soc. Am. Bull. 100 (10), 1578–1593.
Morena, P., Ratzof, G., Cattaneo, A., Klingelhoefer, F., Beck, C., Seibert, C., Marcaillou, B., Feuillet, N., 2022. Coexistence of adjacent siliciclastic, carbonate, and mixed sedimentary systems: an example of seafloor morphology in the Northern Lesser Antilles Forearc. Front. Earth Sci. 10, 834029 doi: 103389/feart.2022.834029.
ODP Leg 110 Scientific Party, 1987. Expulsion of fluids from depth along a subduction-zone decollement horizon. Nature 326 (6115), 785–788.
Patriat, M., Pichot, T., Westbrook, G.K., Umber, M., Deville, E., Benard, F., Roest, W.R., Loubrieu, B., the ANTIPLAC Cruise Party, 2011. Evidence for Quaternary convergence across the North America–South America plate boundary zone, east of the Lesser Antilles. Geology 39 (10), 979–982.
Peterson, L.C., Haug, G.H., 2004. Variability in the mean latitude of the Atlantic Intertropical Convergence Zone as recorded by the riverine input of sediments to the Cariaco Basin (Venezuela). Palæogeogr. Plæoclimatol. Palæoecol. 234, 97–113.
Pichot, T., Patriat, M., Westbrook, G.K., Nalpas, T., Gutscher, M.A., Roest, W.R., Deville, E., Moulin, M., Aslanian, D., Rabineau, M., 2012. The Cenozoic tectonostratigraphic evolution of the Barracuda Ridge and Tiburon Rise, at the western end of the North America–South America plate boundary zone. Mar. Geol. 303–306, 154–171.
Reimer, P., Austin, W., Bard, E., Bayliss, A., Blackwell, P., Bronk Ramsey, C., Butzin, M., Cheng, H., Edwards, R., Friedrich, M., Grootes, P., Guilderson, T., Hajdas, I., Heaton, T., Hogg, A., Hughen, K., Kromer, B., Manning, S., Muscheler, R., Palmer, J., Pearson, C., van der Plicht, J., Reimer, R., Richards, D., Scott, E., Southon, J., Turney, C., Wacker, L., Adolphi, F., Büntgen, U., Capano, M., Fahrni, S., Fogtmann-Schulz, A., Friedrich, R., Köhler, P., Kudsk, S., Miyake, F., Olsen, J., Reinig, F., Sakamoto, M., Sookdeo, A., Talamo, S., 2020. The IntCal20 Northern Hemisphere radiocarbon age calibration curve (0–55 cal kBP). Radiocarbon 62.
Roperch, P., Gattacceca, J., Valenzuela, M., Devouard, B., Lorand, J.-P., Arriagada, C., Rochette, P., Latorre, C., Beck, P., 2017. Surface vitrification caused by natural fires in late Pleistocene wetlands of the Atacama Desert. Earth Planet. Sci. Lett. 469, 15–26.
Rull, V., Montoya, E., Vegas-Vilarrúbia, T., Ballesteros, T., 2015. New insights on palaeofires and savannisation in northern South America. Quat. Sci. Rev. 122, 158–165.
Salgado-Labouriau, M.L., 1997. Late Quaternary paleoclimate in the savannas of South America. J. Quat. Sci. 12 (5), 371–379.
Salgado-Labouriau, M.L., Casseti, V., Ferraz-Vicentini, K.R., Martin, L., Soubiès, F., Suguio, K., Turcq, B., 1997. Late Quaternary vegetational and climatic changes in cerrado and palm swamp from Central Brasil. Palæogeogr. Plaæoclimatol. Palæoecol. 128, 215–226.
Seibert, C., Feuillet, N., Ratzov, G., Beck, C., Cattaneo, A., 2020. Seafloor morphology and sediment transfer in the mixed carbonate siliciclastic environment of the Lesser Antilles forearc along Barbuda to St. Lucia. Mar. Geol. 428, 1–29. https://doi.org/10.1016/j.margeo.2020.106242.
Seibert, C., Feuillet, N., Ratzov, G., Beck, C., Morena, P., Johannes, L., Ducassou, E., Cattaneo, A., Goldfinger, C., Moreno, E., Bieber, A., Benâtre, G., Caron, B., Caron, M., Casse, M., Cavailhes, T., Del Manzo, G., Deschamps, C.E., Desiage, P.A., Duboc, Q., Fauquembergue, K., Ferrant, A., Guyard, H., Jacques, E., Laurencin, M., Leclerc, F., Patton Saurel, J.M., St-Onge, G., Woerther, P., 2024. Sedimentary records in the Lesser Antilles fore-arc basins provide evidence of large late Quaternary megathrust earthquakes. Geochem. Geophys. Geosyst. 25, e2023GC011152 https://doi.org/10.1029/2023GC011152.
Siffedine, A., Martin, L., Turcq, B., Volkmer-Ribeiro, C., Soubiès, F., Campello Cordeiro, R., Suguio, K., 2001. Variation of the Amazonian rainforest environment: a sedimentological record covering 30,000 years. Palæogeogr. Plaæoclimatol. Palæoecol. 168, 221–235.
Siffedine, A., Spadano Albuquerque, A.L., Ledru, M.-P., Turcq, B., Knopper, B., Martin, L., Zamboni de Mello, W., Passnau, H., Landim Dominguez, J.M., Campello Cordeiro, R., Abrão, J.J., da Silva Pinto Bittencourt, A.B., 2003. A 21 000 cal years paleoclimatic record from Caçáo Lake, Northern Brazil: evidence from sedimentary and pollen analyses. Palæogeogr. Plaæoclimatol. Palæoecol. 189, 25–34.
Speed, R.L., 1981. Geology of Barbados: Implication for an accretionary origin. Oceanol. Acta 4, 259–265.
Stéphan, J.F., Mercier de Lépinay, B., Calais, E., Tardy, M., Beck, C., Carfantan, J.C., Olivet, J.L., Vila, J.M., Bouysse, P., Mauffret, A., Bourgois, J., Théry, J.M., Tournon, J., Blanchet, R., Dercourt, J., 1990. Paleogeodynamic maps of the Caribbean: 14 steps from Lias to present. Bull. French Geol. Soc. VI, n° 6, pp. 915–919, (14 pl. h. t).
Symithe, S., Calais, E., de Chabalier, J.B., Robertson, R., Higgins, M., 2015. Current block motions and strain accumulation on active faults in the Caribbean. J. Geophys. Res. Solid Earth 120, 3748–3774.